LUT University

Magnetic and magnetotransport properties of carbon nanotubes modified with cobalt

Ovsiienko I., Sedda A., Shpylka D., Len T., Matzui L., Lähderanta E., Solovjov A., Terekhov A., Mirzoiev I.

This is a Author's accepted manuscript (AAM) version of a publication

published by

in American Institute of Physics

DOI: 10.1063/10.0042298

Copyright of the original publication:

© I. Ovsiienko, A. Sedda, D. Shpylka, T. Len, L. Matzui, E. Lähderanta, A. Solovjov, A. Terekhov, and I. Mirzoiev, 2026

Please cite the publication as follows:

This is a parallel published version of an original publication. This version can differ from the original published article.

Fizyka Nyzkykh Temperatur/Low Temperature Physics, 2026, Vol. 52, No. 2, pp. 223–231

Magnetic and magnetotransport properties of carbon nanotubes modified with cobalt

I. Ovsiienko[1], A. Sedda[2,3], D. Shpylka[1], T. Len[1], L. Matzui[1], E. Lähderanta[2], A. Solovjov[2,4,5], A. Terekhov[5], and I. Mirzoiev[5]

[1]*Taras Shevchenko National University of Kyiv, Department of Physics, Kyiv 01601, Ukraine*

[2]*Department of Physics, LUT University, Lappeenranta 53850, Finland*

[3]*Universitat de les Illes Balears, Palma 07122, Spain*

[4]*Institute of Low Temperature and Structure Research, Polish Academy of Sciences, Wroclaw 50-422, Poland*

[5]*B. Verkin Institute for Low Temperature Physics and Engineering of the National Academy of Sciences of Ukraine*

Kharkiv 61103, Ukraine

E-mail: ovsienko@univ.kiev.ua

Received August 15, 2025, published online December 19, 2025

The temperature and field dependencies of magnetization and electrical resistance of bulk samples of multi-walled carbon nanotubes modified with cobalt have been studied. Samples of modified multi-walled carbon nanotubes with 30% mass fraction of cobalt have been obtained by the method of metal reduction from aqueous salt solution. The hysteresis loops and temperature dependence of mass magnetization under field cooling and zero field cooling protocols have been measured for bulk samples of pressed modified multi-walled carbon nanotubes in a temperature interval from 3 to 293 K. The magnetic field dependence of resistance across a range of temperatures 4.2–300 K in two distinct sample orientations (in-plane and out-of-plane) has been studied in a pulsed magnetic field up to 20 T. The study of the temperature dependence of magnetization in field cooling and zero field cooling modes revealed that the blocking temperature for the studied samples of carbon nanotubes modified with cobalt is ≈ 7 K. It is shown that above the blocking temperature, nanosized single-domain cobalt particles are in a superparamagnetic state. Below the blocking temperature, magnetoresistance is determined by a combination of two mechanisms. Relatively large cobalt particles form ferromagnetic regions, causing a giant magnetoresistive effect to appear. Meanwhile, smaller cobalt particles remain superparamagnetic and form a long tail that does not saturate up to the maximum magnetic field.

Keywords: multi-walled carbon nanotubes, magnetoresistance, magnetization, superparamagnetic state, giant magnetoresistive effect, blocking temperature.

1. Introduction.

After their discovery by Iijima in 1991, carbon nanotubes (CNTs) have been considered a catalyst for the next revolution in science and technology [1]. Due to their exceptional mechanical, optical, thermal, and electrical properties, CNTs have attracted significant interest in various fields such as energy storage, next-generation electronic components, biomedicine, and semiconductor devices. The structural diversity of CNTs is strongly influenced by fabrication methods such as chemical vapor deposition, catalytic decomposition, arc discharge, or laser ablation, which in turn impact their crystallinity, chirality, and defect density. These microstructural features significantly affect their low-temperature transport properties, including thermoelectric power, magnetoresistance, and electrical conductivity [2–4]. The magnetic and magnetotransport properties of CNTs can also be modified by the introduction of magnetic impurities such as magnetic metal particles (Fe, Co, or Ni) into the inner cavity or deposited on the surface of CNTs [5–10]. This integration of CNTs with magnetic metal particles significantly changes their intrinsic electrical and magnetic properties [11–13].

Many efforts have been devoted to studying the effect of doping on the magnetic properties of CNTs. In the past, K. Lafdi *et al.* [6] reported that undoped carbon nanotubes

© I. Ovsiienko, A. Sedda, D. Shpylka, T. Len, L. Matzui, E. Lähderanta, A. Solovjov, A. Terekhov, and I. Mirzoiev, 2026

exhibit diamagnetic behavior while Co-doped nanotubes exhibit superparamagnetic behavior with magnetization saturation at about 0.5 T. Authors in [14–15] studied the magnetic characterization of CNTs modified with cobalt as a function of the magnetic field and temperature. Spin-dependent charge transfer in carbon nanotubes modified with magnetic impurities was observed by the authors in a number of works when studying their conductivity in a magnetic field [16–20]. Herein, we investigate the magnetic and magnetotransport properties of carbon nanotubes modified with cobalt, prepared by catalytic decomposition of carbon monoxide, over a wide range of temperatures and magnetic fields.

2. Experimental methods and samples

2.1. Samples fabrication and characterization

The source multi-walled carbon nanotubes (MWCNTs) were synthesized via low-temperature catalytic decomposition of carbon monoxide. Modification of MWCNTs with cobalt has been carried out by reducing the metal from a water-salt solution in a hydrogen flow. The method of modifying MWCNTs with cobalt is described in detail in [13]. The calculated cobalt mass content in the MWCNTs was 30%.

Figure 1 shows fragments of scanning electron microscope (SEM) images of the modified MWCNTs studied. The sample studied consists of elongated cylindrical structures with a diameter of up to 150 nm. The sample also contains individual nanotube intergrowths with a diameter of up to 5 μm. However, at this magnification, cobalt particles are not visible on the surface of the MWCNTs.

The crystal structure and phase composition of modified MWCNTs at ambient temperature were examined using a PANalytical Empyrean 3 diffractometer (Co tube, $\lambda = 0.1789$ nm) equipped with a hybrid monochromator (parabolic mirror + double bounce Ge(220) monochromator) for the incident beam and a PIXcel3D-Medipix3 detector for the diffracted beam. The beam size was chosen to cover the entire surface of the sample. Figure 2 shows a fragment of the X-ray diffraction pattern for the modified MWCNTs.

As can be seen from Fig. 2, one intense broadened 002-graphite band and several bands corresponding to cobalt and its oxides are observed in the diffractogram. The exact angular position of the 002-graphite band corresponds to the interplanar distance $d_{002} = 0.344$ nm. The crystallite size L determined from the graphite band broadening according to the Scherrer formula is ~ 4 nm. These parameters of the MWCNTs structure are close to the values of the crystalline structure parameters for disordered (amorphous) graphite materials. The sufficiently intense narrow lines in the diffractogram are associated with reflection from the atomic planes of hexagonal cobalt. The values of the sizes of the coherent scattering blocks determined from the broadening of these lines are equal to ≈ 20 nm. In addition, the diffractogram contains two weakly intense lines, indicating the presence of cobalt oxides CoO and Co_3O_4 in the sample.

Therefore, the sample studied is multi-walled carbon nanotubes of imperfect structure, modified with hexagonal cobalt particles. The tubes also showed the presence of small amounts of cobalt oxides CoO and Co_3O_4.

2.2. Preparation of bulk samples of modified multilayer carbon nanotubes for magnetic and magneto-transport measurements

For the preparation of bulk samples, the powder of modified MWCNTs was mixed with polyvinyl acetate and sonicated in an aqueous medium for 30 min. The prepared mixture was dried in air at room temperature until complete removal of moisture. The bulk samples of modified MWCNTs were made by cold pressing of the prepared mixture at room temperature and a pressure of 100 MPa in the form of rectangular parallelepipeds. The dimensions of the samples are 2 × 3.5 × 15 mm, and the density is ≈ 1.75 g/cm^3. In bulk samples, as previous studies have shown, there is a

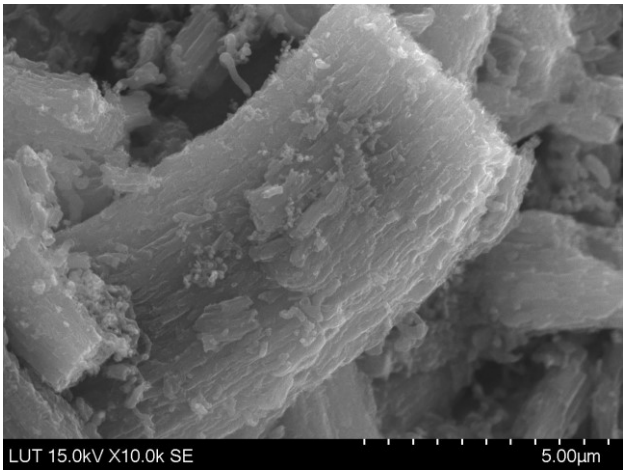

(a)

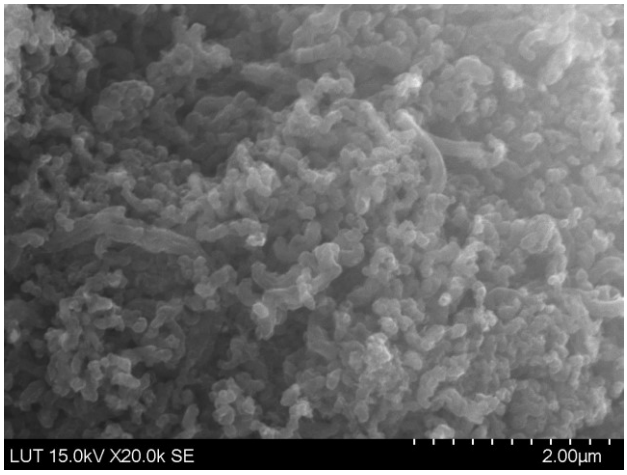

(b)

Fig. 1. Fragments of SEM images of the studied modified MWCNTs, (a) and (b) show different regions at varying magnifications.

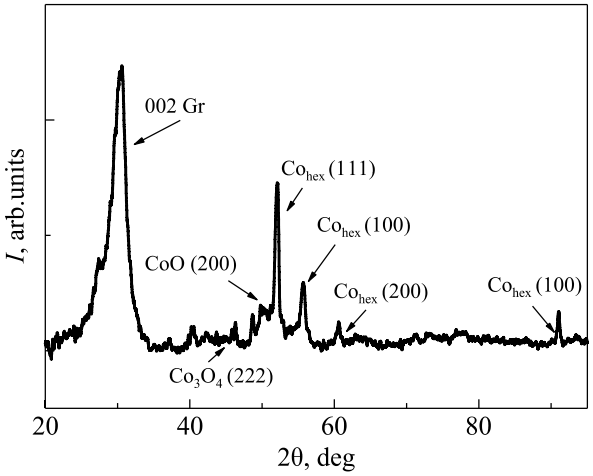

Fig. 2. Fragment of the X-ray diffraction pattern for the modified MWCNTs.

certain orientation of carbon nanotubes. The nanotubes are oriented in such a way that their axes are mainly in the plane perpendicular to the direction of pressing [21].

2.3. Measurements of magnetization and resistance in magnetic field

The hysteresis loops and temperature dependence of mass magnetization under field cooling (FC) and zero field cooling (ZFC) protocols in the in-plane orientation were measured using a SQUID magnetometer (Cryogenic S700X).

Resistance measurements in a magnetic field were performed using the pulsed magnetic field setup (PMFS) technique, employing the standard four-probe method with one pair of current probes and one pair of voltage probes. This configuration was used to investigate the magnetic field dependence of resistance across a range of temperatures 4.2–300 K and in two distinct sample orientations: in-plane and out-of-plane. A pulsed magnetic field of 20 T, with a duration of 12 ms, was applied during the measurements. Magnetoresistance has been defined as the ratio of the resistance change in the magnetic field to the resistance in the zero field: $\frac{\rho(B)-\rho(0)}{\rho(0)} = \frac{\Delta\rho}{\rho}$. The measurement error of the resistance did not exceed 0.1%.

3. Experimental results

3.1. Experimental studies of magnetization of modified multi-walled carbon nanotubes

According to the methods described above, studies of the temperature dependence of magnetization under FC and ZFC protocols were conducted. Figure 3 shows the temperature dependencies of magnetization $M(T)$ under FC and ZFC protocols in magnetic fields of 5 mT, 50 mT, and 0.5 T. As can be seen in the figure, the dependence of $M(T)$ in both measurement modes for all applied magnetic fields can be divided into two sections: up to a certain temperature, the magnetization decreases slightly (Sec. I), and then its

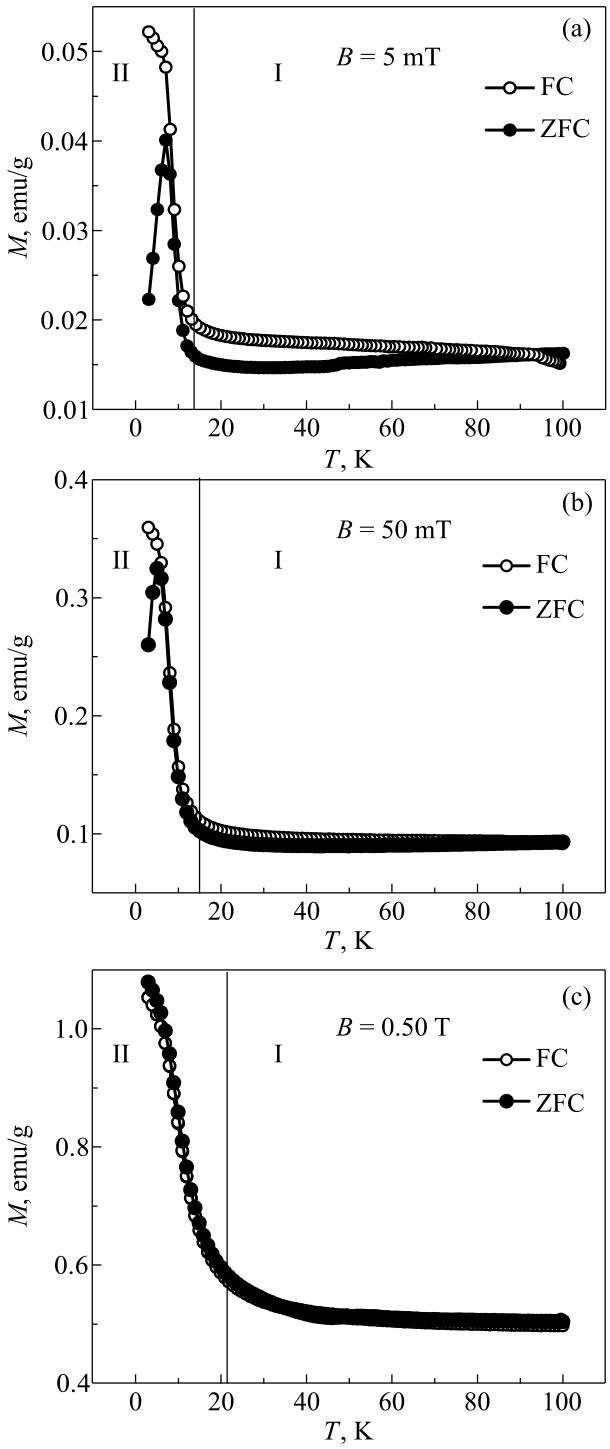

Fig. 3. Temperature dependencies of magnetization $M(T)$ under FC and ZFC protocols for modified MWCNTs in magnetic fields 5 mT (a), 50 mT (b), and 0.5 T (c).

sharp increase is observed (Sec. II). The temperature at which the sharp increase in magnetization begins is higher in larger magnetic fields. In Sec. I, the temperature dependence of magnetization is similar under the FC and ZFC protocols. However, as the temperature decreases further, the temperature dependencies of magnetization under the FC and ZFC protocols diverge. Magnetization in the FC mode increases

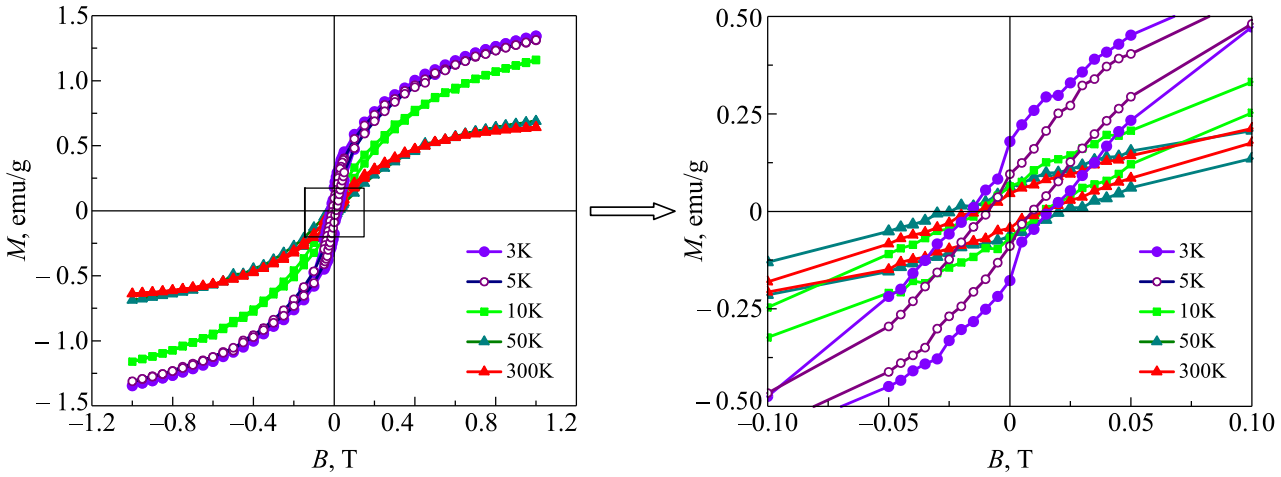

Fig. 4. (Color online) Dependencies $M(B)$ for a bulk sample of modified MWCNTs in the temperature interval from 3 to 300 K.

with decreasing temperature over the entire studied range, whereas magnetization in the ZFC mode begins to drop sharply once a certain temperature is reached. The temperature at which this drop begins decreases with increasing applied magnetic field. In a magnetic field of 5 mT, the temperature at which the maximum in the $M(T)$ dependence under the ZFC protocol occurs is 7.05 K. In a magnetic field of 50 mT, the maximum in the $M(T)$ dependence in ZFC mode shifts to a lower temperature region and is accordingly 5.1 K. For an applied magnetic field of 0.5 T, the decrease in magnetization in the ZFC mode is not observed in the temperature range in which the measurements were performed [Fig. 3(c)]. However, as can be seen in the figure, the $M(T)$ dependencies under the FC and ZFC protocols start to diverge.

Figure 4 presents the hysteresis loops of a bulk sample of modified MWCNTs at temperatures ranging from 3 to 300 K. As seen in the figure, magnetization increases as the temperature decreases. At the same time, saturation of the magnetization is not achieved at any measurement temperature in a field up to 1 T.

Figure 5 shows the temperature dependencies of the residual magnetization M_r and coercive force B_c for a bulk sample of modified MWCNTs.

According to Fig. 5, the residual magnetization M_r increases with decreasing temperature, and a sharp increase of M_r is observed at temperatures below 5 K, so the dependence correlates with the results shown in Fig. 3. The dependence of the coercive force B_c on temperature is less obvious. When the temperature is decreased to 50 K, the coercive force increases slightly, with a further decrease in temperature, however, the coercive force decreases.

3.2. *Experimental studies of electrical resistance in magnetic field*

Figure 6 shows the temperature dependence of the resistivity for a bulk sample of MWCNTs modified with cobalt. For comparison, the figure also shows the temperature dependence of the resistivity for the source for modification multi-walled CNTs.

As can be seen from the figure, the resistivity of the bulk sample of the source for modification of MWCNTs decreases with increasing temperature, which is typical for MWCNTs. The ratio $\rho_{4.2}/\rho_{293}$ for the source MWCNTs is ~2.79. Modifying the source MWCNTs does not change the nature of the temperature dependence of the resistivity;

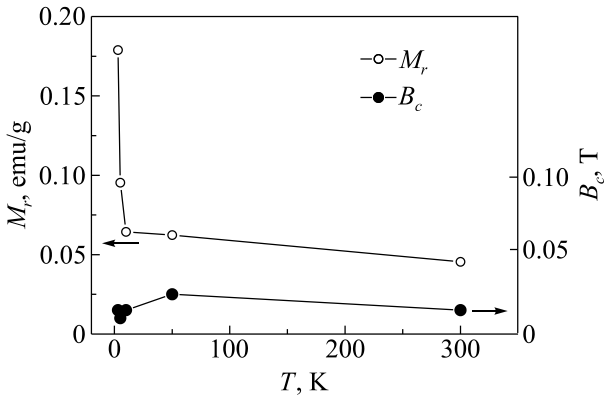

Fig. 5. Temperature dependencies of the residual magnetization M_r and coercive force B_c for a bulk sample of MWCNTs modified with cobalt.

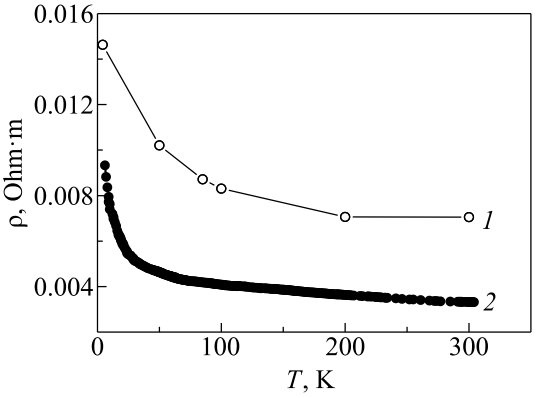

Fig. 6. Temperature dependencies of the resistivity for a bulk sample of MWCNTs modified with cobalt (*1*) and the source for modification MWCNTs (*2*).

however, the $\rho_{4.2}/\rho_{293}$ ratio for the modified MWCNTs decreases slightly to ~2.1, which is close to the values $\rho_{4.2}/\rho_{293}$, for example, fine-crystalline anisotropic graphite [22]. However, modifying the source MWCNTs leads to an increase by a factor of 1.5–2 in the resistivity (Fig. 6). Similar changes in resistivity for bulk samples of MWCNTs were observed, for example, in [20] after modification of carbon nanotubes with iron and in [23] after intercalation of MWCNTs with cobalt. Such an increase in the resistivity following modification appears to be primarily associated with an increase in the contact electrical resistance between the individual CNTs and the particles of metal.

Therefore, modifying the source MWCNTs with cobalt and its compounds, with a significant mass concentration of up to 30%, does not result in the formation of a continuous metallic cluster within the bulk MWCNT sample.

Figure 7 shows the dependencies of the transverse (out-of-plane geometry) and longitudinal (in-plane geometry) magnetoresistance on the magnetic field in the temperature range 4.2–300 K for bulk samples of MWCNTs modified with cobalt.

As illustrated in the figure, the transverse and longitudinal magnetoresistances are both negative at all measurement temperatures. The only exception is the transverse magnetoresistance at a temperature of 300 K. In the interval of magnetic fields up to 2 T, the magnetoresistance changes sign, and a local maximum is observed in the dependence $\Delta\rho/\rho = f(B)$ at $B = 1$ T. For all other measurement temperatures, such a change in sign is not observed for either the transverse or longitudinal magnetoresistance. The form of the dependence $\Delta\rho/\rho = f(B)$ for transverse magnetoresistance in the temperature range from 200 to 50 K is similar. In a magnetic field of up to 5 T, the dependence $\Delta\rho/\rho = f(B)$ is quadratic, but in higher fields, there is a transition to linear dependence. Note that magnetoresistance saturation is not observed in magnetic fields up to 20 T in the temperature range from 300 to 50 K. The absolute values of transverse magnetoresistance increase as the temperature decreases. A qualitative and quantitative change in dependence $\Delta\rho/\rho = f(B)$ is observed at a temperature of 4.2 K. The absolute value of the magnetoresistance at the maximum field is approximately eight times greater than the transverse magnetoresistance value at 50 K. The form of the magnetoresistance field dependence also changes. The linear section of the $\Delta\rho/\rho = f(B)$ dependence is only observed in small magnetic fields. As the magnetic field increases further, the magnetoresistance changes slightly, but saturation of the dependence $\Delta\rho/\rho = f(B)$ is not observed. The values of the longitudinal magnetoresistance for the bulk sample of modified MWCNTs are only slightly lower than those of the transverse magnetoresistance.

4. Discussion of experimental results

As the structural-phase studies show, the samples under study represent a complex, heterogeneous system whose components have different magnetic properties. The source for the modification, multi-walled carbon nanotubes, like all carbon materials, are diamagnetic. Modified MWCNTs

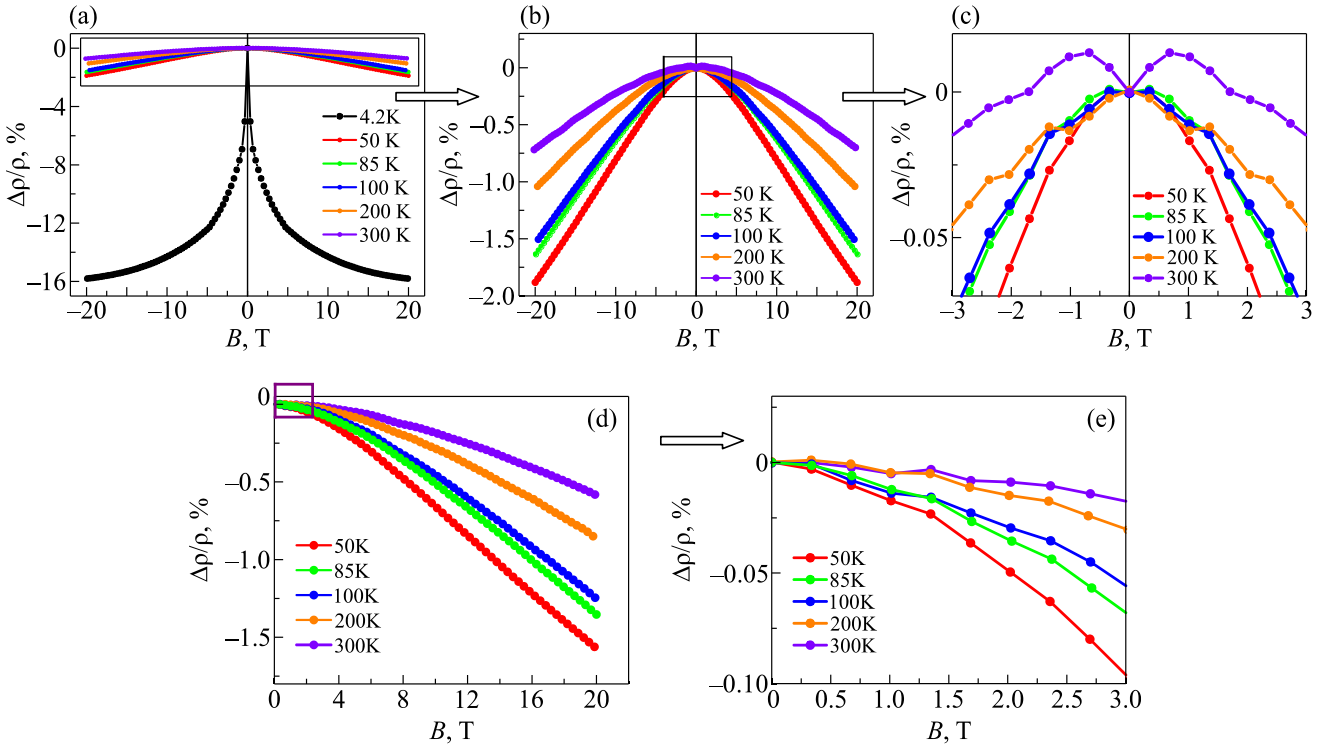

Fig. 7. (Color online) Transverse (a)–(c) and longitudinal (d)–(e) magnetoresistance for bulk samples modified with cobalt MWCNTs at different temperatures.

contain two magnetic phases: hexagonal cobalt and cobalt oxide (CoO), which is an antiferromagnet with a Neel temperature of 291 K. This means that the transition to the antiferromagnetic state occurs almost at room temperature. According to the X-ray diffraction data, the average size of the cobalt and cobalt oxide particles is ≈ 20 nm, and they appear to be located both on the surface and in the internal cavity of the CNTs.

Let us analyze in detail the features of the magnetic and magnetotransport properties of modified MWCNTs.

Studies have shown that the magnetization curves under the FC and ZFC protocols below a certain temperature have different temperature dependencies. In the FC regime, the $M(T)$ curve increases continuously with decreasing temperature. In the ZFC regime, the $M(T)$ curve exhibits a maximum, the position of which depends on the applied magnetic field. At an applied magnetic field of 5 mT, the maximum in the $M(T)$ dependence in the ZFC mode occurs at ≈ 7 K, and with increasing applied magnetic field, the maximum in the $M(T)$ dependence shifts to the lower temperature region. This difference in $M(T)$ dependence between ZFC and FC modes is typical of magnetic materials in a superparamagnetic state.

As is known, superparamagnetism is manifested for nanosized ferromagnetic particles that are in a single-domain state. Ferromagnetic nanoparticles exhibit magnetic anisotropy. Consequently, their magnetic moment exhibits only two stable collinear orientations that are parallel to an axis known as the axis of easy magnetization. The magnetization direction of nanoparticles is caused to flip randomly by thermal fluctuations. For single-domain, non-interacting particles, the average time between two magnetization vector flips, known as the Néel relaxation time τ_N, is determined from the Néel–Arrhenius equation [24]:

$$\tau_N = \tau_0 e^{\frac{KV}{k_B T}}, \quad (1)$$

where τ_0 is the characteristic relaxation time, which is determined by many factors, in particular, the temperature of the system, the gyromagnetic state, the value of the anisotropy constant, the height of the energy barrier, and other factors, K is the magnetic anisotropy energy density of a nanoparticle, V is the volume of nanoparticle, thus, KV is the energy barrier for the rotation of the magnetization vector. If the temperature is high enough, $KV/k_bT << 1$, the time τ_N required for the system to transition to the equilibrium state is very small compared to the characteristic time τ_m of measuring the magnetic characteristics. Therefore, for a system containing nanosized particles in the superparamagnetic state at high temperatures, the magnetization does not saturate, and hysteresis is not observed. If $KV/k_bT >> 1$, the time τ_N to reach the equilibrium state will be long enough, and the orientation of the magnetic moments of the particles will be preserved during the measurement. The temperature at which the measurement time τ_m is equal to the time for the system to reach the equilibrium state (relaxation time τ_N) is defined as the blocking temperature T_b. The blocking temperature T_b is experimentally determined as the point at which the temperature dependence of magnetic susceptibility diverges in the FC and ZFC regimes. From Eq. (1) under the condition $\tau_m = \tau_N$, the blocking temperature is determined as

$$T_b = \frac{KV}{k_b \ln\left(\frac{\tau_m}{\tau_0}\right)}. \quad (2)$$

Considering that the characteristic time of static magnetic measurements $\tau_m = 100$ s and $\tau_0 = 10^{-9}$ s [22], Eq. (2) can be presented in the form

$$T_b = \frac{KV}{25k_b}, \quad (3)$$

or the diameter d of the magnetic phase particles can be estimated as

$$d = \left(\frac{150 T_b k_b}{\pi K}\right)^{\frac{1}{3}}. \quad (4)$$

According to Eq. (4), using experimental data on the temperature dependence of magnetization (Fig. 3) and the value of the energy density of magnetic anisotropy K for spherical hexagonal cobalt nanoparticles [25], the diameter of cobalt particles was estimated to be ≈ 6 nm. This is slightly smaller than the size of the cobalt particles, as determined by X-ray diffraction. The discrepancy in the sizes of cobalt particles, as determined by temperature-dependent magnetization and XRD data, may be due to some heterogeneity and dispersion in cobalt particle size. In any case, however, cobalt particles are single-domain since, according to work [25], the critical size of the transition of cobalt nanoparticles to the single-domain state is 70 nm.

Therefore, according to the experimental data, nanosized single-domain cobalt particles on the surface and within the internal cavity of CNTs are in a superparamagnetic state. At a temperature of 7 K, the magnetic moments of the cobalt nanoparticles are locked. Let us analyze the experimental data on the magnetization and magnetoresistance of CNTs modified with cobalt within this framework.

As shown in Fig. 7, in the temperature range 300–50 K, the absolute value of magnetoresistance increases linearly with increasing magnetic field. It does not reach saturation at the maximum magnetic field at which the studies were conducted. At the same time, the absolute values of magnetoresistance in the same magnetic fields increase as the temperature decreases. These temperature and field dependencies of magnetoresistance are characteristic of a magnetic system in a superparamagnetic state, which is defined by an almost linear increase in magnetoresistance absolute value with an increasing applied magnetic field and an absence of saturation even in large magnetic fields. However,

the situation changes radically at a temperature of 4.2 K, i.e., below the locking temperature of magnetic moments, as determined by the temperature dependence of the magnetization, which is equal to ≈ 7 K.

As in previous cases, magnetoresistance does not saturate at the maximum measurement field. However, the magnetoresistance value decreases by ≈ 12% in magnetic fields up to 5 T. With an increase in magnetic field to 20 T, the absolute magnetoresistance value changes by only 4%. Therefore, two regions can be distinguished on the MR curves: the central region, where magnetoresistance decreases rapidly from 0 to 12%, and the region from 5 to 20 T, where magnetoresistance decreases significantly less. Such a complex field dependence of magnetoresistance at a temperature of 4.2 K can be assumed to be due to the superposition of two magnetoresistance mechanisms associated with different magnetic states of cobalt particles. The shape of the dependence $\Delta\rho/\rho(B)$ in a magnetic field up to 5 T (i.e., the central part of the dependence) is characteristic of the giant magnetoresistance (GMR) effect. However, the magnitude of the GMR effect itself is much smaller than that observed for iron-modified MWCNTs in [5]. Clearly, at a given temperature, a certain fraction of relatively large cobalt particles forms ferromagnetic regions that can be interconnected through a layer of antiferromagnetic cobalt oxide, which is also present in CNTs, as can be seen from the X-ray diffraction data. At the same time, smaller cobalt particles at this temperature remain in a superparamagnetic state and, accordingly, form a long tail that does not saturate up to the maximum magnetic field of measurement.

These assumptions are confirmed by data from the study of hysteresis loops for a bulk sample of modified MWCNTs at different temperatures (Fig. 4). As can be seen in the figure, the magnitude of magnetization increases with decreasing temperature, but no saturation of magnetization is observed at any temperature in the range of magnetic fields for which the studies were conducted.

As is known, the resistance of a system consisting of dispersed, randomly distributed magnetic clusters in a nonmagnetic matrix can be given as [26]:

$$R = r\left(1 \pm \alpha J + \beta J^2\right), \qquad (5)$$

where r is the resistance arising from spin-independent scattering, J is the s–d exchange interaction, α and β are some constants, and the sign of the linear term depends on the direction of the electron spin. In a material containing magnetic particles in a superparamagnetic state, the linear term is averaged out, and the magnetoresistance only contains a second-order term in J. The presence of ferromagnetic particles breaks the spin symmetry and causes the conduction electrons to become spin polarised. This leads to the appearance of a first-order term in Eq. (5) for macroscopic resistance. This alters the shape and magnitude of the magnetoresistance. The magnetization of the magnetic particles determines the field dependence of the first-order term in J.

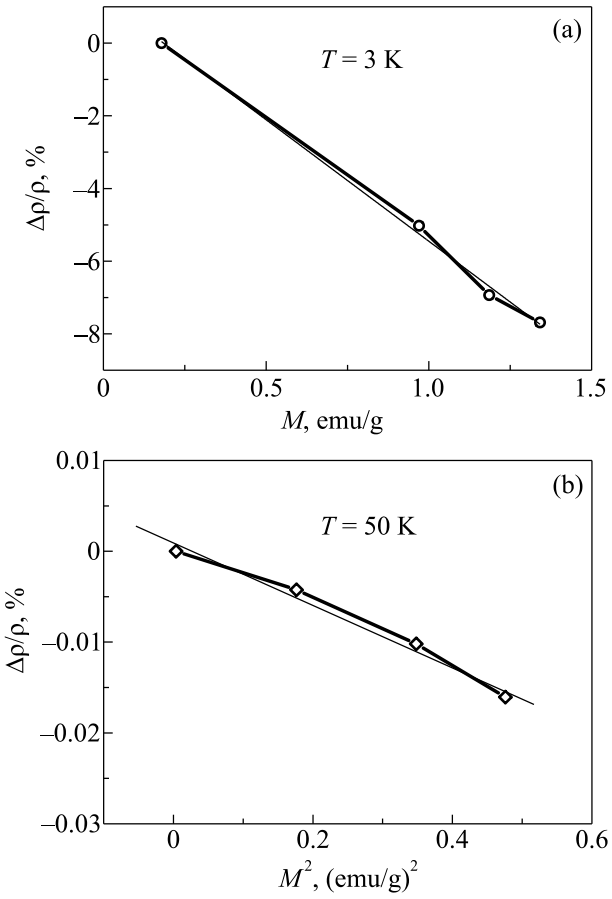

Fig. 8. Dependencies $\Delta\rho/\rho = f(M)$ at $T = 3$ K and $\Delta\rho/\rho = f(M^2)$ at $T = 50$ K for a bulk sample of modified MWCNTs.

Figure 8 shows the dependence of magnetoresistance $\Delta\rho/\rho$ on the magnitude of magnetization M at a temperature of 3 K, as well as the dependence of magnetoresistance $\Delta\rho/\rho$ on the square of magnetization M^2 at a temperature of 50 K. As illustrated, the dependence $\Delta\rho/\rho = f(M)$ is linear at a temperature of 3 K, and a deviation from linearity only occurs in the maximum field in which magnetization studies were carried out. At 50 K, the dependence $\Delta\rho/\rho$ on the square of the magnetization is almost linear. Therefore, at low temperatures, the linear term in the expression (5), which is associated with the spin-dependent scattering of charge carriers on magnetically oriented cobalt particles, makes a significant contribution to the resistance in a magnetic field. Above the blocking temperature, however, spin-independent scattering of charge carriers on chaotically magnetically oriented cobalt particles in a superparamagnetic state takes place.

5. Conclusions

Studies have revealed that multi-walled carbon nanotubes modified with cobalt are a complex, heterogeneous system comprising components in various magnetic states. In the diamagnetic matrix, which is multi-walled CNTs, ferromagnetic cobalt nanoparticles and a small amount of antiferromagnetic cobalt oxide (CoO) particles are distributed. The combination of phases in different magnetic states in

one system leads to the emergence of new magnetic and magnetotransport properties of such a system.

Studies of the temperature dependence of magnetization revealed that the magnetization in FC mode increases at different rates with decreasing temperature, while the temperature dependence of magnetization obtained in ZFC mode contains a pronounced maximum. The presence of a maximum in the temperature dependence of magnetization upon cooling of the system in the ZFC mode indicates the locking of the magnetic moments of nanosized single-domain cobalt particles, which were in a superparamagnetic state above the blocking temperature.

Measurements of hysteresis loops also confirm the superparamagnetic state of cobalt nanoparticles on/in MWCNTs above the blocking temperature.

The magnetoresistance of multi-walled carbon nanotubes modified with cobalt above the blocking temperature also exhibits field and temperature dependence characteristic of a granular system in a superparamagnetic state. The magnetoresistance is negative, and its absolute value increases as the temperature decreases. Throughout the range of magnetic fields studied, up to 20 T, magnetoresistance does not saturate. Below the blocking temperature, magnetoresistance is determined by a combination of two mechanisms. Relatively large cobalt particles form ferromagnetic regions that can be interconnected via a layer of antiferromagnetic cobalt oxide. This causes the appearance of a giant magnetoresistive effect, which is observed in magnetic fields up to 5 T as a sharp decrease in magnetoresistance. At the same time, smaller cobalt particles at this temperature remain in a superparamagnetic state and, accordingly, form a long tail that does not saturate up to the maximum magnetic field of measurement.

Acknowledgments

L. Matzui and I. Ovsiienko acknowledge the financial support from the National Research Foundation of Ukraine, grant NRFU2023-03/193. The work was supported by the Academy of Finland, grant numbers 343309 and 367561 and by the National Academy of Sciences of Ukraine within the scientific program F19-5. A. Solovjov thanks the Department of Physics, LUT University, Lappeenranta, Finland, for their hospitality. The authors also thank Santeri Kurkinen (LUT Separation Science Department) for the SEM analysis.

1. *Carbon Nanotubes: Synthesis, Structure, Properties, and Applications*, M. Dresselhaus, G. Dresselhaus, and P. Avouris (eds.), Springer Berlin, Heidelberg (2001).
2. C. Zhou, J. Kong, E. Yenilmez, and H. Dai, *Science* **290**, 1552 (2000).
3. R. Tarkiainen, M. Ahlskog, J. Penttilä, L. Roschier, P. Hakonen, M. Paalanen, and E. Sonin, *Phys. Rev. B* **64**, 195412 (2001).
4. J.-C. Charlier, X. Blase, and S. Roche, *Rev. Mod. Phys.* **79**, 677 (2007).
5. D. O. Shpylka, I. V. Ovsiienko, T. A. Len, L. Yu. Matzui, S. V. Trukhanov, A. V. Trukhanov, and O. S. Yakovenko, *Ceram. Int.* **48**, 19789 (2022).
6. K. Lafdi, A. Chin, N. Ali, and J. F. Despres, *J. Appl. Phys.* **79**, 6007 (1996).
7. H. Shiozawa, A. Briones-Leon, O. Domanov, G. Zechner, Yu. Sato, K. Suenaga, T. Saito, M. Eisterer, E. Weschke, W. Lang, H. Peterlik, and T. Pichler, *Sci. Rep.* **5**, 15033 (2015).
8. A. Jensen, J. R. Hauptmann, J. Nygård, and P. E. Lindelof, *Phys. Rev. B* **72**, 035419 (2005).
9. J. Kim, J.-R. Kim, J. W. Park, Ju-Jin Kim, K. Kang, N. Kim, and B.-Ch. Woo, *Physica E* **18**, 208 (2003).
10. D. Shpylka, I. Ovsiienko, T. Len, L. Matzui, Yu. Prylutskyy, and T. Tsaregradskaya, *Proceedings of the 2023 IEEE 13th International Conference "Nanomaterials: Applications and Properties"*, NAP 2023, Bratislava, Slovakia (2023).
11. I. Krainov, J. Klier, A. Dmitriev, S. Klyatskaya, M. Ruben, W. Wernsdorfer, and I. Gornyi, *ACS Nano* **11**, 6868 (2017).
12. S. Krompiewski, R. Gutierrez, and G. Cuniberti, *Phys. Rev B* **69**, 155423 (2004).
13. I. Ovsienko, T. Len, L. Matzui, Yu. Prylutskyy, P. Eklund, F. Normand, U. Ritter, and P. Scharff, *Physica E* **37**, 78 (2007).
14. G. E. Grechnev, V. A. Desnenko, A. V. Fedorchenko, A. S. Panfilov, Y. I. Prylutskyy, M. I. Grybova, L. Y. Matzui, U. Ritter, P. Scharff, and Y. A. Kolesnichenko, *Materialwiss. Werkstofftech.* **42**, 29 (2011).
15. U. Ritter, P. Scharff, G. E. Grechnev, V. A. Desnenko, A. V. Fedorchenko, A. S. Panfilov, Yu. I. Prylutskyy, and Yu. A. Kolesnichenko, *Carbon* **49**, 4443 (2011).
16. B. W. Alphenaar, K. Tsukagoshi, and H. Ago, *Physica E* **6**, 848 (2000).
17. B. W. Alphenaar, K. Tsukagoshi, and M. Wagner, *Physica E* **10**, 499 (2001).
18. K. Tsukagoshi and B. W. Alphenaar, *Superlattices Microstruct.* **27**, 565 (2000).
19. H. Tokoro, S. Fujii, and T. Oku, *Diamond Relat. Mater.* **13**, 1270 (2004).
20. I. V. Ovsienko, L. Y. Matzui, I. V. Yatsenko, S. V. Khrapatiy, Y. I. Prylutskyy, U. Ritter, P. Scharff, and F. Le Normand, *Materialwiss. Werkstofftech.* **44**, 161 (2013).
21. I. V. Ovsiienko, L. L. Vovchenko, L. Yu. Matzui, T. L. Tsaregradskaya, T. A. Len, G. V. Saienko, and V. M. Geraskevych, *Springer Proceed. Phys.* **279**, 347 (2023).
22. O. I. Prokopov, I. V. Ovsiienko, L. Yu. Matzui, T. A. Len, D. D. Naumova, I. B. Berkutov, I. G. Mirzoiev, and F. Le Normand, *Low Temp. Phys.* **43**, 703 (2017) [*Fiz. Nizk. Temp.* **43**, 884 (2017)].
23. I. V. Ovsiienko, T. A. Len, L. Yu. Matzui, F. L. Normand, T. L. Tsaregradskaya, G. V. Saenko, and D. O. Spylka, *Mol. Cryst. Liquid Cryst.* **718**, 80 (2021).
24. O. Redon, J. Pierre, B. Rodmacq, B. Mevel, and B. Dieny, *J. Magn. Magn. Mater.* **149**, 398 (1995).
25. Yu. O. Tykhonenko-Polishchuk and A. I. Tovstolytkin, *J. Nano- Electron. Phys.* **9**, 02028 (2017).
26. M.-T. Béal-Monod and R. A. Weiner, *Phys. Rev.* **170**, 552 (1968).

Магнітні та магнітотранспортні властивості модифікованих кобальтом вуглецевих нанотрубок

I. Ovsiienko, A. Sedda, D. Shpylka, T. Len, L. Matzui, E. Lähderanta, A. Solovjov, A. Terekhov, I. Mirzoiev

Досліджено температурну та польову залежності намагніченості та електричного опору об'ємних зразків багатостінних модифікованих кобальтом вуглецевих нанотрубок. Зразки модифікованих багатостінних вуглецевих нанотрубок із 30% масовою часткою кобальту були отримані методом відновлення металу з водно-сольового розчину. Було виміряно петлі гістерезису та температурну залежність масової намагніченості за протоколами охолодження в магнітному полі та без нього для об'ємних зразків пресованих модифікованих багатостінних вуглецевих нанотрубок у температурному інтервалі від 3 до 293 К. Залежність опору від магнітного поля в діапазоні температур 4,2–300 К у двох різних орієнтаціях зразків (площинній та позаплощинній) було досліджено в імпульсному магнітному полі до 20 Т. Дослідження температурної залежності намагніченості в режимах охолодження в магнітному полі та без нього показало, що температура блокування для досліджуваних зразків модифікованих кобальтом вуглецевих нанотрубок становить ≈ 7 К. Показано, що вище температури блокування нанорозмірні однодоменні частинки кобальту знаходяться в суперпарамагнітному стані. Нижче температури блокування магнітоопір визначається комбінацією двох механізмів. Відносно великі частинки кобальту утворюють феромагнітні області, що призводить до появи гігантського магніторезистивного ефекту. Тим часом менші частинки кобальту залишаються суперпарамагнітними та утворюють довгий хвіст, який не насичується до максимального магнітного поля.

Ключові слова: багатостінні вуглецеві нанотрубки, магнітоопір, намагніченість, суперпарамагнітний стан, гігантський магніторезистивний ефект, температура блокування.